Chaos
An Interdisciplinary Journal of Nonlinear Science

RESEARCH ARTICLE | MAY 09 2023

Direction-dependent noise-induced synchronization in mobile oscillators

Special Collection: Disruption of Networks and System Dynamics

Emilda Shajan ; Dibakar Ghosh ; Jürgen Kurths ; Manish Dev Shrimali

Chaos 33, 053108 (2023)
https://doi.org/10.1063/5.0146983

Direction-dependent noise-induced synchronization in mobile oscillators

Cite as: Chaos 33, 053108 (2023); doi: 10.1063/5.0146983
Submitted: 17 February 2023 · Accepted: 11 April 2023 ·
Published Online: 9 May 2023

Emilda Shajan,[1] Dibakar Ghosh,[2] Jürgen Kurths,[3] and Manish Dev Shrimali[1,a)]

AFFILIATIONS

[1]Department of Physics, Central University of Rajasthan, Ajmer 305817, Rajasthan, India
[2]Physics and Applied Mathematics Unit, Indian Statistical Institute, 203 B. T. Road, Kolkata 700108, India
[3]Potsdam Institute for Climate Impact Research, Potsdam 14473, Germany

Note: This paper is part of the Focus Issue on Disruption of Networks and System Dynamics.
[a)]**Author to whom correspondence should be addressed:** shrimali@curaj.ac.in

ABSTRACT

Synchronization among uncoupled oscillators can emerge when common noise is applied on them and is famously known as noise-induced synchronization. In previous studies, it was assumed that common noise may drive all the oscillators at the same time when they are static in space. Understanding how to develop a mathematical model that apply common noise to only a fraction of oscillators is of significant importance for noise-induced synchronization. Here, we propose a direction-dependent noise field model for noise-induced synchronization of an ensemble of mobile oscillators/agents, and the effective noise on each moving agent is a function of its direction of motion. This enables the application of common noise if the agents are oriented in the same direction. We observe not only complete synchronization of all the oscillators but also clustered states as a function of the ensemble density beyond a critical value of noise intensity, which is a characteristic of the internal dynamics of the agents. Our results provide a deeper understanding on noise-induced synchronization even in mobile agents and how the mobility of agents affects the synchronization behaviors.

In most of the previous studies on noise-induced synchronization, the oscillators were assumed static in space and common noise was applied to all the oscillators uniformly at the same time. This results in a single cluster of a completely synchronized oscillator. However, in the scenario of mobile oscillators in motion governed by the Vicsek model, we observe the emergence of multiple synchronized clusters which can be tuned by varying the ensemble density. The proposed model employs a noise field which enables the application of common noise depending on the direction of orientation of the mobile agents in the physical space. The average size of completely synchronized clusters as a function of the ensemble density follows a power-law distribution. The scheme is successfully implemented using the PR circuit model, the HR neuron model, and a Gaussian map as the internal dynamics of the mobile agents.

I. INTRODUCTION

Being the most significant and interesting emergent phenomenon, synchronization is that facet of dynamical systems that is given unparalleled attention and importance in research.[1] Direct or indirect communications between uncorrelated oscillators, even chaotic ones, attain a state of complete or phase synchronization within a short span of time after initialization. The obvious occurrence of such phenomena in both natural and artificial situations justifies the need to study them in detail in networks as well, where a large number of identical or non-identical oscillators are interacting through various kinds of coupling schemes, resulting in several collective behaviors, including synchronization,[2] amplitude or oscillation death,[3,4] chimera states,[5–9] etc. These networks can be classified according to the nature of the edges connecting the nodes. The topology can either be fixed in time with a predefined adjacency matrix[10,11] or can be evolving in time.[12–14]

Apart from the classical models of networks with fixed or dynamic topologies, there is another class of networks known as mobile oscillators/agents, which are primarily inspired from real life scenarios of social and communication networks, epidemiology, and other biological and engineering systems.[15–18] They are characterized by the coordinates of the moving agents in the physical space, and interactions are active only within a defined neighborhood. Each agent is also associated with an internal dynamics evolving

in its corresponding state space. Such a moving neighborhood network having Rössler oscillator dynamics were observed to attain synchronization[19] with the individual agents employing a random walk. The impact of different time scales for the physical motion and internal dynamics was also examined[20] in a similar way. A study on a time-evolving network of Kuramoto oscillators associated with mobile agents in diffusive motion was also found to end up in a synchronized state.[21] There were more research on mobile oscillators that touch upon specific features, such as amplitude death,[22] fast switching synchronization,[23,24] and explosive synchronization.[25,26] Multiplex networks with moving agents were also noted to have intra- and interlayer synchronization behavior.[27] A model in which attractive or repulsive coupling is chosen based on the relative distance between the agents was another study on synchronization in mobile oscillator systems.[28] Recently, another work was done considering a direct mutual influence between the dynamics in both the physical and state space.[29]

The strategy adapted for the motion of the mobile agents in space can impact the outcome as well as the physical significance. For example, the vision range of the agents is often considered only in the forward direction as it is more realistic in real life situations, such as traffic and the movement of fireflies.[22] Even though random walk strategies are very commonly used to describe the motion of the agents in space, the Vicsek model[30] can be another realistic alternative to it. In this framework, the particles move along the average orientation of the nearby particles, which is perturbed by thermal noise as well. The tendency of the individual units in motion to get influenced by its neighbors is described well in this framework. This is known to give rise to characteristic motion patterns, which are sensitive to the particle density in the physical space as well as transportation. The method was utilized in a bunch of problems previously in mobile oscillators[31,32] and have inspired similar works on swarmalators also.[33–36]

Synchronization of uncoupled oscillators using noise of specific intensity is an explored aspect of noise-induced phenomena in dynamical systems. Noise-induced complete synchronization was achieved in two identical Lorenz attractors, while phase synchronization happens in non-identical attractors.[37] According to the studies carried out on various maps and flows,[38] noise is responsible for pushing the individual trajectories into the contraction region of the system under consideration, eventually leading to complete synchronization of the trajectories. It was also observed that the time spent by the trajectories in the contraction region can be improved by restricting the noise infusion to a limited range of the state space resulting in an enhanced synchronization.[39] Realistic systems, such as the Pikovski–Rabinovich (PR) circuit model and the Hindmarsh–Rose (HR) neuron model, also show noise-induced synchronization.[40] In fact, neuron models are known to have high sensitivity to channel noises.[41] The phenomenon of noise-induced synchronization can be analyzed effusively by the largest conditional Lyapunov exponent, which assumes a negative value if the synchronization is feasible.[42] It is to be noted that most of the investigation of noise-induced synchronization observed in uncoupled oscillators is considering the oscillators to be static in space. Noise-induced synchronization in mobile oscillators is unexplored to date to the best of our knowledge in spite of the possible practical applications of it, especially in engineering fields.[43,44]

In this paper, we implement a strategy of noise-induced synchronization in mobile oscillators, which are moving in the physical space in accordance with the Vicsek model, each carrying an internal oscillator dynamics. Unlike the previous works on mobile oscillators, here, we do not employ any coupling interactions between the agents. Instead, the agents are allowed to move in a noise field in such a way that the effective noise on each agent is a function of the direction of orientation of the velocity vector associated with it. This causes the noise experienced to be common for only those agents that are oriented in the same direction. Hence, complete synchronization of all the mobile oscillators is possible only when the density of agents in space is beyond a threshold causing mutually parallel motion of the agents in space. For intermediate values of density, we observe synchronized clusters of oscillators as well, which can be attributed to multiple domains that are formed with their own direction of orientation common within each domain. We discuss the general form of the proposed scheme in Sec. II. The illustration of the scheme is done using the PR circuit model as an example of the nodal dynamics in Sec. III A along with a detailed analysis of the same. Sections III B and III C verify the applicability of the proposed method in two more systems, which are the HR neuron model and a 1D Gaussian map, respectively. Finally, we do a conclusive discussion in Sec. IV.

II. THE PROPOSED MATHEMATICAL MODEL

Let us consider a set of N mobile agents in a physical space specified by the coordinates $(\zeta_i, \xi_i) \in \mathbb{R}^2$, where $i = 1, 2, \ldots, N$. The motion of the agents is governed by the Vicsek model[30] and obeys periodic boundary conditions. The density of agents in space is $\rho = N/L^2$, where L is the edge length of the physical space. The numerical calculation of the motion of these agents is given by

$$\begin{aligned}(\zeta_i, \xi_i)(t + \Delta t) &= (\zeta_i, \xi_i)(t) + v\hat{\mathrm{v}}_i(t)\Delta t,\\ \theta_i(t + \Delta t) &= \langle \theta_{i'}(t)\rangle_r + \Delta\theta,\end{aligned} \tag{1}$$

where v is the scalar magnitude of velocity with which the agents move and θ_i is the angle of orientation of the unit velocity vector $\hat{\mathrm{v}}_i = (\cos\theta_i, \sin\theta_i)$. The angle θ_i of any agent at each time step $\Delta t = 1$ is given by the average of that of the neighboring agents, $\theta_{i'}$, within a circle of radius r with an additional thermal perturbation $\Delta\theta$ chosen randomly from a uniform distribution $[-\kappa/2, \kappa/2]$. Here, κ is the perturbation intensity. We keep $r = 1$ and analyze the system as a function of the density ρ.

Now, we assign an internal dynamics to each of the mobile agents along with a noise vector $\eta(t) = \eta_\zeta \hat{\zeta} + \eta_\xi \hat{\xi}$ acting on them, where η_ζ and η_ξ are two noise components drawn from Gaussian distributions of zero mean and unit variance. The dynamics of individual agents is given by

$$\dot{X}_i = F(X_i) + A\varepsilon\hat{\mathrm{v}}_i(t) \cdot \eta_i(t). \tag{2}$$

Here, $X = \{x_j\} \in \mathbb{R}^n$ is the n-dimensional state vector of the individual agents $(i = 1, \ldots, N)$ having an intrinsic dynamics $F(X) = \{f(x_j)\}$. $A = \{A_j\}, j = 1, 2, \ldots, n$ is an array where $A_j = \begin{cases} 1 & \text{if } j = m, \\ 0 & \text{otherwise}, \end{cases}$ and x_m is the state variable in which the noise

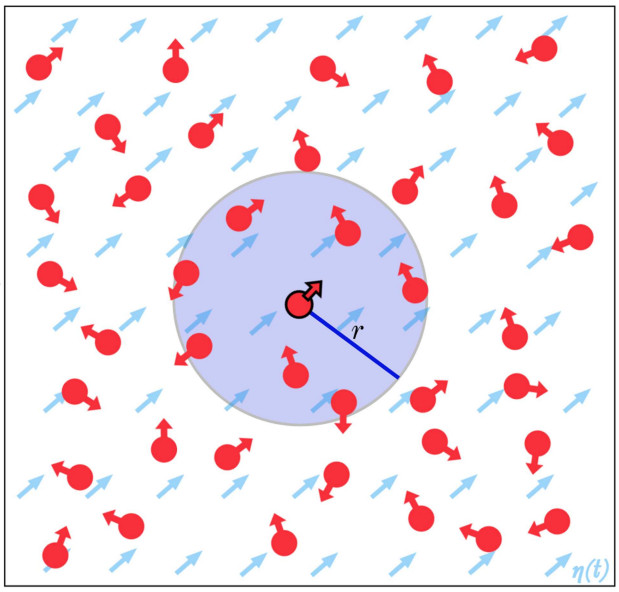

FIG. 1. Schematic representation of the movement of N mobile oscillators oriented at $\theta_i, i = 1, \ldots, N$ (red arrows) in a 2D physical space of area L^2. The angle of orientation of each agent is affected by the average angle of orientation of the neighboring agents within a circle of radius r. $\eta(t)$ is the noise field of strength ε applied (blue arrows).

$\eta(t)$ of intensity ε acts. The dot product $\varepsilon\hat{\mathrm{v}}_i(t) \cdot \eta_i(t)$ indicates the component of noise along the direction of orientation of the individual mobile agents. The range of ε and the choice of x_m can be specific to the internal dynamics attributed to the individual agents. The direction in which the applied noise can cause synchronization is dependent on the structure of the contraction region associated with the oscillators, which is the key to attaining noise-induced synchronization.[37] A schematic representation of the model is shown in Fig. 1.

III. RESULTS

We verify the proposed mathematical model for noise-induced synchronization between uncoupled mobile oscillators by considering three different systems, namely, the chaotic Pikovski–Rabinovich circuit model, the slow–fast Hindmarsh–Rose neuron model, and a one-dimensional Gaussian map.

A. Pikovski–Rabinovich circuit model

We first illustrate the whole model with the Pikovski–Rabinovich (PR) circuit model[45] taken as the internal dynamics of the individual agents. We modify Eq. (2) by replacing $F(X_i)$ with the equations of motion of the PR system,

$$\begin{aligned} \dot{x}_i &= y_i - \alpha z_i, \\ \dot{y}_i &= -x_i + 2\beta y_i + \gamma z_i, \\ \dot{z}_i &= (x_i - z_i^3 + z_i)/\delta + \varepsilon\hat{\mathrm{v}}_i \cdot \eta(t), \end{aligned} \tag{3}$$

with $\alpha = 0.66$, $\beta = 0.201$, $\gamma = 0.165$, and $\delta = 0.047$. The noise is added in the z component, which is the optimal direction to attain synchronization in a PR system.[40] Taking $\nu = 0.03, \kappa = 0.001$, $\rho = 1.0$, and $\varepsilon = 4.0$, we see that all the N number of PR oscillators with random initial conditions get completely synchronized with increasing noise intensity as shown in Fig. 2. Figure 2(a) shows the time series of the y variable of the $N = 100$ oscillators with zero noise intensity, which is nothing but the intrinsic dynamics of the PR oscillators. However, at an elevated noise intensity $\varepsilon = 4$, all the oscillators get synchronized with each other in time [Fig. 2(b)]. Note that this phenomenon of complete synchronization of all the mobile agents is possible only when the internal dynamics of each of the agents is subjected to common noise of sufficient intensity. Considering the fact that the mobile oscillators in our model are moving in an anisotropic noise field, this condition of common noise can be fulfilled only when all the agents are oriented in the same direction in physical space. It is a characteristic feature of the Vicsek model[30] that allows self-organization to a single direction of orientation at a sufficiently high density of particles. Figure 2(c) quantifies the synchronization error $\langle E \rangle = \sum_{i=2}^{N} |X_i - X_1|/(N-1)$, where $|X_i - X_1|(i = 2, 3, \ldots, N)$ are the absolute errors with X_1, with increase in the noise strength ε. We observe that the synchronization error goes to zero beyond critical noise strength $\varepsilon_c = 3.0$. It is also evident from the figure that ε_c is mostly independent on the size of the system N under consideration. In Fig. 2(d), we analyze the dependence of the occurrence of synchronization on the set of initial conditions of the mobile oscillators. It is analyzed in terms of the basin stability,[46] S_B, of the completely synchronized state, which is nothing but the ratio of the volume of the state space that converges into the synchronized state to the total volume of the state space considered. Here, we can see that beyond the critical noise intensity, the system attains synchronization irrespective of the choice of initial conditions as $S_B = 1$. It is also to be noted that for a much higher noise intensity, the oscillator dynamics goes unbounded as well. The largest Lyapunov exponent (LLE) of the oscillations can be monitored as a tool to infer the occurrence of the transition to the completely synchronized state in Fig. 2(e) as the LLE goes from positive to negative at the critical noise intensity for synchronization in agreement with the basin stability curve.

We shall also examine the effect of the density ρ of the moving agents in the physical space, on the order that is being induced in the internal dynamics of the oscillators due to the noise field. As we know already that the Vicsek model gives rise to unidirectional transportation at high density, it is also observable that the moving agents can form multiple domains, each oriented in a random direction. However, even in this case, the individual oscillators belonging to the same domain experience common noise and, hence, achieve synchronization. This gives rise to multiple synchronized clusters in the internal dynamics.

Figure 3 presents a pictorial account of the above-mentioned results. The plots in the three columns from left to right represent the three cases of $\rho = 0.001, 0.1$ and 2.0 with $\varepsilon = 4.0$. The first row of plots shows snapshots of the position and orientation of the mobile agents in the physical space. The angle of orientation θ of the agents ranging from $-\pi$ to π is represented as a color bar. The second row depicts the spatiotemporal plots of the individual oscillators associated with the agents, and the third row gives snapshots of the y

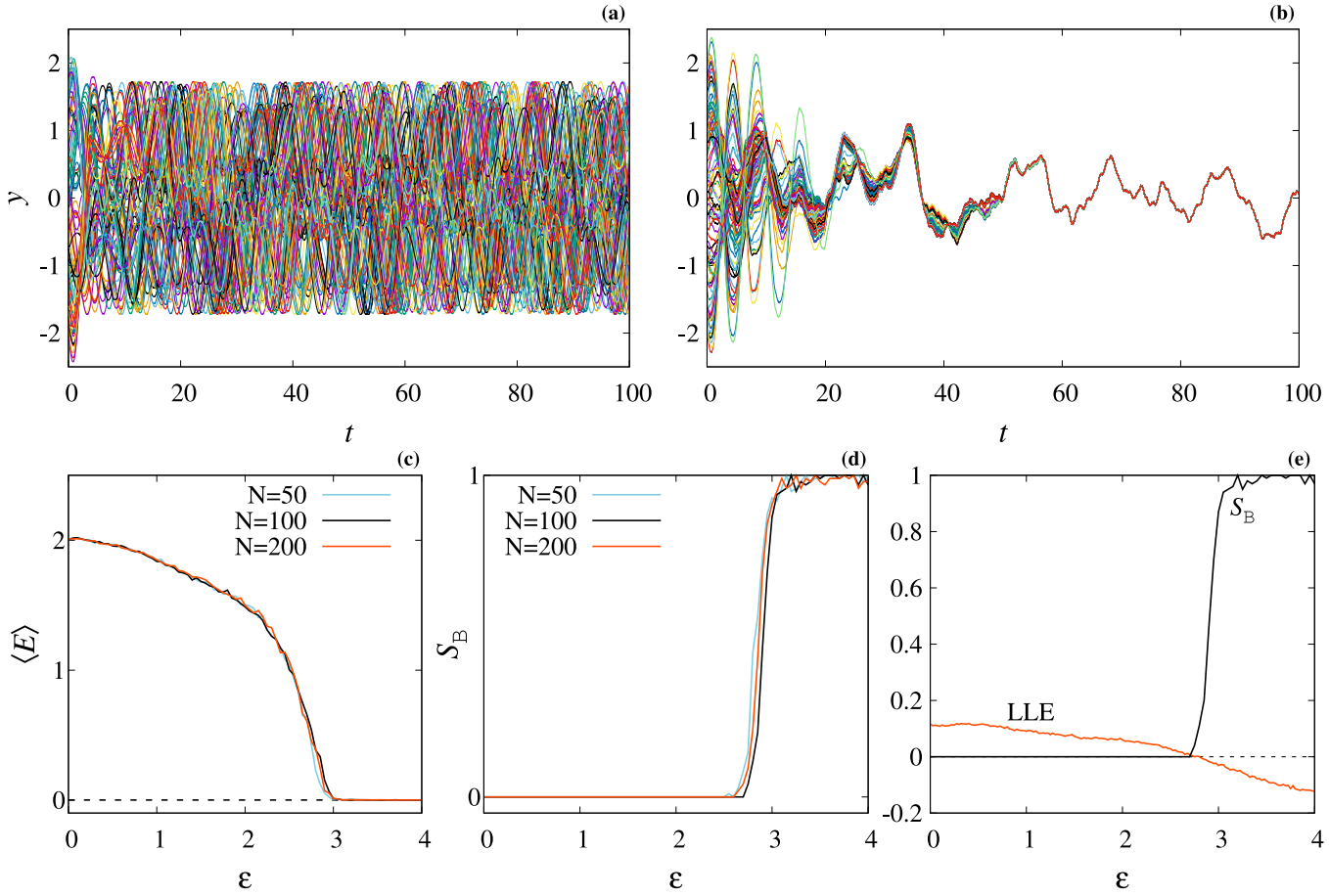

FIG. 2. Time series of the mobile oscillators in Eq. (3) with (a) $\varepsilon = 0.0$, desynchronized state and (b) $\varepsilon = 4.0$, synchronized state. The variation of the (c) synchronization error $\langle E \rangle$ and (d) basin stability S_B as a function of the noise intensity ε for various system sizes. (e) Largest Lyapunov exponent as a function of the noise strength ε plotted along with the basin stability. Density is kept constant at $\rho = 1.0$ for all the plots.

variables of the mobile oscillators. For a low density, the agents move almost randomly, as it is visible in Fig. 3(a), and the internal dynamics shows no sign of synchronization as we can see in Figs. 3(d) and 3(g). However, at a moderate value of density, in Fig. 3(b), we see multiple domains of agents, each having a common orientation. This gives rise to multiple clusters of completely synchronized oscillations in the internal dynamics of the agents [Figs. 3(e) and 3(h)]. In the third case of high density of agents, all the agents orient themselves in the same direction over time [Fig. 3(c)], and all the oscillators arrive at a state of complete synchronization as we had discussed previously, which can be observed from Figs. 3(f) and 3(i) as well. Multimedia views of all three cases in Figs. 3(a)–3(c) are available.

Furthermore, in Fig. 4(a), we see that, with a continuous increment in the density ρ with a sufficiently high $\varepsilon = 4.0$, the average number of synchronized clusters shows an exponential decrement settling down to a single cluster beyond a critical value $\rho = \rho_c = 1.5$. This implies that the noise experienced by the mobile oscillators beyond this critical density is identical for all the agents, thus causing the formation of a single synchronized cluster. Furthermore, on an analysis of the average size of the synchronized clusters, $\langle CS_{sync} \rangle$, we identify power-law behavior. $\langle CS_{sync} \rangle \sim (\rho - \rho_c)^{-\gamma}$, with the exponent $\gamma = 0.68$. The corresponding log–log plot in Fig. 4(b) follows a straight line with a slope $-\gamma$ in the transition region. The effect of density on the completely synchronized state can be justified by inspecting the mutual information[47] between a pair of randomly chosen oscillators in the ensemble calculated by the formula

$$MI = \sum_{i,j}^{N_t} P(i,j) log \frac{P(i,j)}{P(i)P(j)},$$

where $P(i)$ and $P(j)$ are the individual probabilities of occurrence of the two oscillators in the ith and jth volume cells in the phase space and $P(i,j)$ is the probability of the combined occurrence of them and N_t is the total number of time steps considered. A close look at the

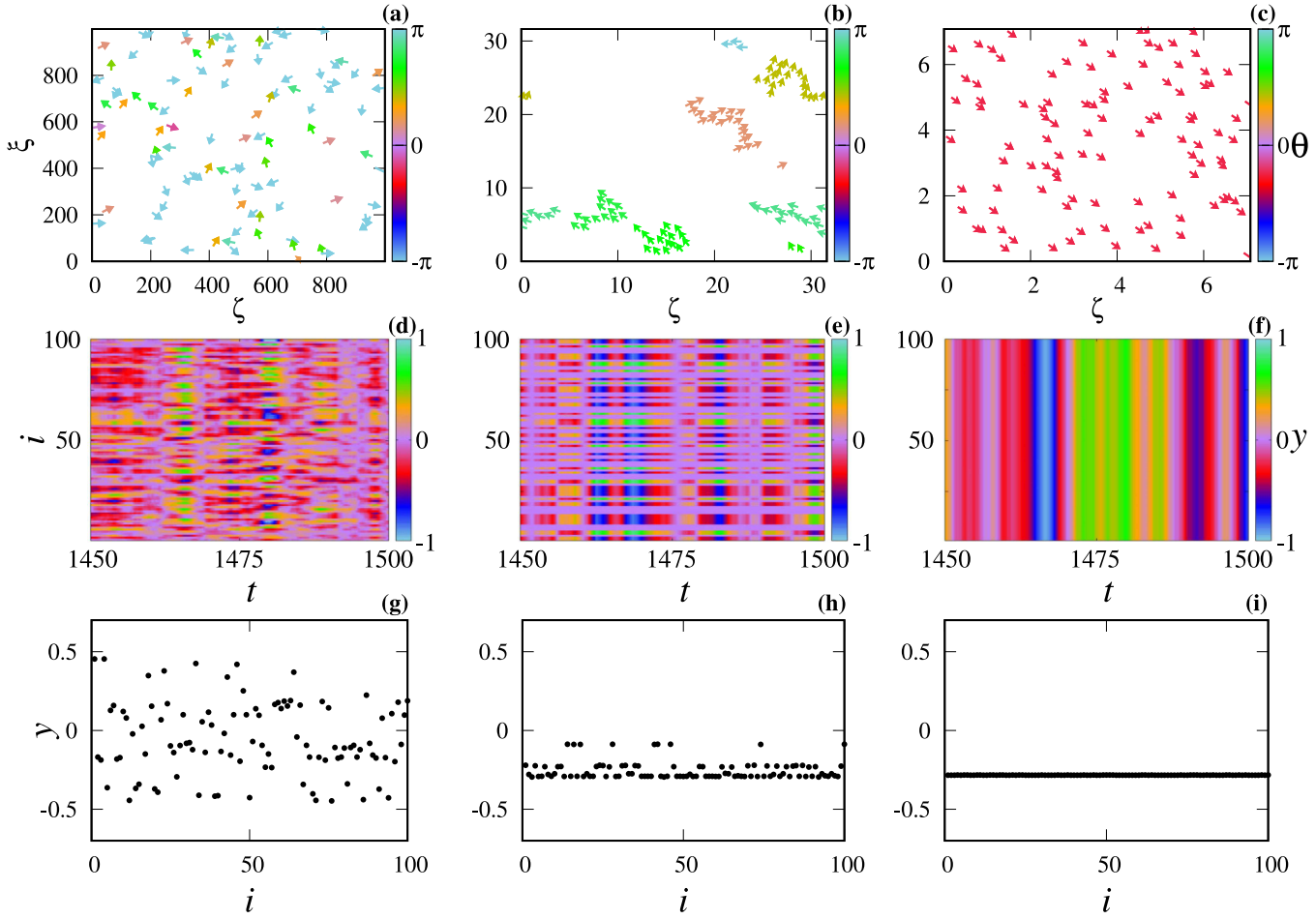

FIG. 3. (a)–(c) Snapshots of the position and orientation of the mobile agents in Eq. (3) in the physical space under various ensemble densities. The corresponding video files showing the evolution of the ensembles with $\rho = 0.0001$ in (a), $\rho = 0.1$ in (b), and $\rho = 2.0$ in (c) are also available. (d)–(f) Spatiotemporal plots of the mobile oscillators. (g)–(i) Snapshots of the y variable of the individual oscillators with index i corresponding to the ensembles in (a)–(c). Here, $\varepsilon = 4.0$. Multimedia views: https://doi.org/10.1063/5.0146983.1; https://doi.org/10.1063/5.0146983.2; https://doi.org/10.1063/5.0146983.3

plot in Fig. 4(c) will reinforce our observation as the critical density ρ_c corresponds to a maximum value of the mutual information and remains constant thereafter. We also examine the system in the various parameter planes in terms of the basin stability as well. We plot the $(\varepsilon - \rho)$, $(\rho - r)$, and $(\rho - v)$ parameter planes. The $(\varepsilon - \rho)$ parameter plane [Fig. 4(d)] reveals a range of ε over which complete synchronization of all the mobile agents occurs. Apart from this range, the oscillators are unsynchronized for low values of noise strength, while get unbounded for higher values. We also observe the existence of the threshold density of mobile agents beyond which all the agents experience common noise to facilitate a completely synchronized state, which is in agreement with the critical density of agents for a single cluster formation according to Fig. 4(a). Similarly, Fig. 4(e) shows the $(\rho - r)$ parameter plane in which we observe the threshold value of r required for complete synchronization of all the oscillators as a function of the density ρ. Provided a minimum threshold condition is satisfied, the higher the density, the lower the value of the critical r necessary for synchronization. Figure 4(f) shows the $(\rho - v)$ parameter space, and it is clear from the map that for a density beyond $\rho = 1.5$, even the practically immobile ensemble of oscillators will also get synchronized. While for a lower density, the synchronization is possible only if the agents are moving with an appreciable velocity v.

B. Hindmarsh–Rose neuron model

We now successfully execute the scheme on another chaotic system to verify the applicability of the proposed method. The motion of the agents in the physical space and the noise infusion strategy are kept the same, while the internal dynamics of the agents is replaced by the Hindmarsh–Rose (HR) neuron model.[48] Neural systems are known to have effects, such as stochastic resonance from

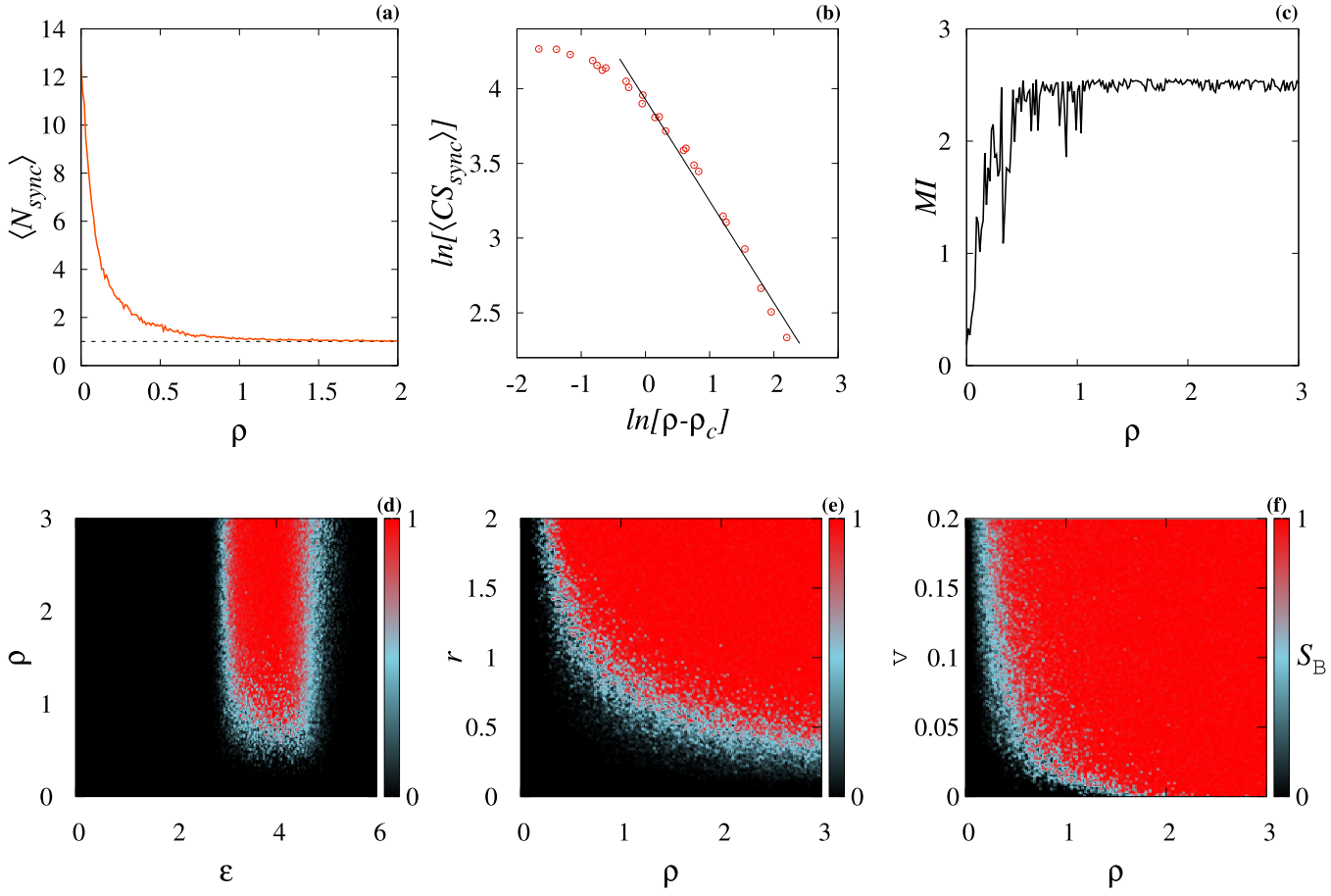

FIG. 4. (a) The average number of synchronized clusters, (b) the log–log plot of the average size of synchronized clusters, and (c) the average mutual information between a pair of randomly chosen oscillators from the ensemble as a function of the density of mobile agents in Eq. (3) at $\varepsilon = 4.0$. Variation of basin stability S_B by varying simultaneously two parameters in (d) $(\varepsilon - \rho)$, (e) $(\rho - r)$, and (f) $(\rho - v)$ parameter space maps.

different biologically relevant noises.[49,50] Identical HR oscillators are already known to synchronize under the influence of common noise. We modify their intrinsic dynamics by adding the direction-dependent noise term in the x direction, which is optimal for the HR model.[40] The modified dynamics is, thus, given by

$$\begin{aligned} \dot{x}_i &= y_i - \alpha x_i^3 + \beta x_i^2 - z_i + I + \varepsilon \hat{\mathrm{v}}_i \cdot \eta(t), \\ \dot{y}_i &= \gamma - \delta d x_i^2 - y_i, \\ \dot{z}_i &= \zeta [S(x_i - \chi) - z_i], \end{aligned} \tag{4}$$

where $\alpha = 1.0$, $\beta = 3.0$, $\gamma = 1.0$, $\delta = 5.0$, $\zeta = 0.006$, $S = 4.0$, $\chi = -1.56$, and $I = 3.0$. We attain a completely synchronized state with this model as well at similar ranges of mobile oscillator density but a different critical noise intensity as it is characteristic solely of the internal dynamics of the oscillators. In Fig. 5(a), with at $\rho = 2.0$, we identify that the critical noise density in this case is $\varepsilon = 2.5$, indicating the onset of complete synchronization of all the mobile oscillators. At this critical point, the synchronization error graces zero, and simultaneously, the basin stability curve reaches 1 assuring the independence of the synchronization on the choice of initial conditions. Figure 5(b) shows the (ε, ρ) parameter plane, indicating the broader range of noise density over which the synchronized state is stable for the HR model. However, one can see that the threshold density of mobile oscillators required for complete synchronization remains the same as it is the basic requirement to assure the exertion of common noise.

C. Gaussian map

Finally, we adapted the model to test the scheme with a 1D Gaussian map as well, which is given by[51]

$$x_i(n+1) = b\alpha x_i(n) exp\left[-2x_i(n)^2 + a x_i(n)\right] + \varepsilon \hat{\mathrm{v}}_i \cdot \eta(t), \tag{5}$$

where $\alpha = \sqrt{e}/2, a = 0, b = 7$. Similar to the previous cases, a complete synchronized state is attained for sufficiently high density $\rho = 1.5$, and in Fig. 5(c), the synchronization error curve as well as

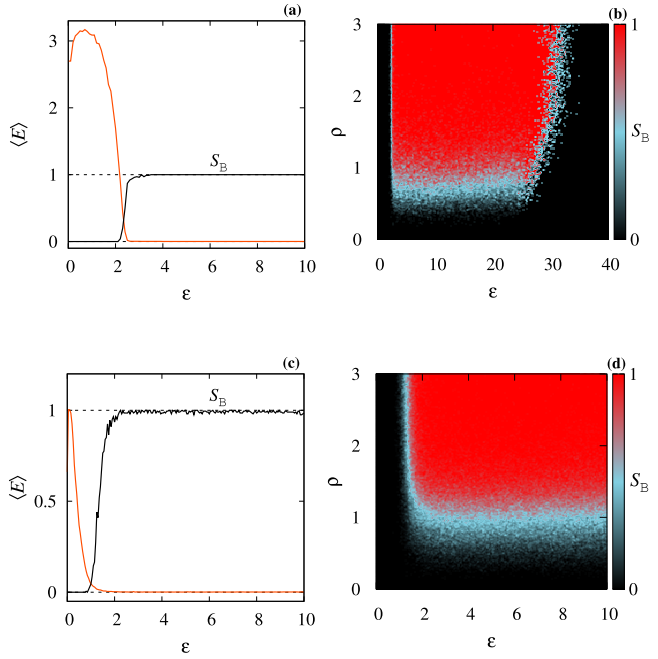

FIG. 5. Synchronization error $\langle E \rangle$ and basin stability S_B variation as a function of noise strength ε at $\rho = 2.0$ and the $(\varepsilon - \rho)$ parameter space basin stability map, respectively, for (a) and (b) the HR neuron model [Eq. (4)] and for (c) and (d) Gaussian map [Eq. (5)].

the basin stability curve show the transition to complete synchronization at $\varepsilon = 1.9$ for $\rho = 2.0$. Compared to the previous case, the noise intensity required for complete synchronization of the ensemble is appreciably less in the case of the map considered. However, in Fig. 5(d), the (ε, ρ) parameter plane indicates a deviation from the previous cases as the dynamics of the oscillators are found to remain synchronized for higher values of noise strengths without going unbounded. It can be attributed to the nature of the map considered that the synchronized state remains stable even for very high noise strengths without getting unbounded.

IV. CONCLUSION

In this work, we have formulated and executed a strategy to synchronize the internal dynamics of an ensemble of mobile oscillators with their motion in the physical space governed by the Vicsek model. We have investigated synchronization among uncoupled moving oscillators when a direction-dependent noise field is introduced in such a way that the individual oscillators experience common noise if they are oriented parallel to each other. We have found that the ensemble attains complete synchronization on the application of the noise field of appropriate noise strength when the density of the mobile agents in space is beyond a critical value. These two critical values (noise intensity and density of mobile agents) depend on the internal dynamics of the agents. By the nature of the motion described by the Vicsek model with a circular neighboring region of radius r, we have seen no synchronization for a low density of agents as the agents are oriented randomly. However, for a moderate value of density, the formation of domains of agents having the same orientation takes place forming multiple synchronized clusters. Finally, after a critical value of agent's density, we obtained a complete synchronization state as all the agents get oriented parallel with each another and common noise has been applied to all the agents at the same time. Therefore, by increasing the density of the agents in the physical space, the chances of common noise on more agents increase. By this way, the direction of the movement increases rapidly when the density of the agents increases in the physical space.

To verify our claim, we used the PR circuit model as the internal dynamics of the mobile agents for a detailed illustration of the model and later extended the study to the HR neuron model as well as to a Gaussian map to ensure the universality of the scheme. The PR model was studied to show the formation of multiple synchronized clusters eventually forming a single synchronized cluster (complete synchronization) on the gradual increment of the density of the mobile agents. The transition to a completely synchronized state was identified to be in agreement with the switching of the sign of the largest Lyapunov exponent to negative over gradation of noise intensity. The influence of the model parameters, such as the density of mobile agents ρ, the radius of interaction in the Vicsek model r, and the velocity of motion of the agents v, was analyzed in terms of the basin stability. Using the above three dynamical systems as the internal dynamics of the agents, we conclude that the critical value of noise strength for complete synchronization depends on the internal dynamics. Moreover, the ensemble density plays a pivotal role in determining the number of synchronized clusters. With the backup of our findings, we expect our model to find adaptive applications in various fields, especially in wireless sensors, mobile *ad hoc* networks, etc.

ACKNOWLEDGMENTS

D.G. was supported by the Department of Science and Technology, Government of India (Project No. CRG/2021/005894).

AUTHOR DECLARATIONS

Conflict of Interest

The authors have no conflicts to disclose.

Author Contributions

Emilda Shajan: Formal analysis (lead); Investigation (lead); Methodology (lead); Validation (lead); Visualization (lead); Writing – original draft (lead). **Dibakar Ghosh:** Conceptualization (equal); Funding acquisition (equal); Project administration (equal); Supervision (equal); Validation (equal); Visualization (equal); Writing – review & editing (equal). **Jürgen Kurths:** Conceptualization (equal); Project administration (equal); Supervision (equal); Validation (equal); Visualization (equal); Writing – review & editing (equal). **Manish Dev Shrimali:** Conceptualization (equal); Project administration (equal); Supervision (equal); Validation (equal); Visualization (equal); Writing – review & editing (equal).

DATA AVAILABILITY

The data that support the findings of this study are available within the article.

REFERENCES

[1] A. Pikovsky, M. Rosenblum, and J. Kurths, *A Universal Concept in Nonlinear Sciences* (Cambridge University Press, 2001).
[2] A. Arenas, A. Díaz-Guilera, J. Kurths, Y. Moreno, and C. Zhou, "Synchronization in complex networks," Phys. Rep. **469**, 93–153 (2008).
[3] G. Saxena, A. Prasad, and R. Ramaswamy, "Amplitude death: The emergence of stationarity in coupled nonlinear systems," Phys. Rep. **521**, 205–228 (2012).
[4] A. Koseska, E. Volkov, and J. Kurths, "Oscillation quenching mechanisms: Amplitude vs. oscillation death," Phys. Rep. **531**, 173–199 (2013).
[5] D. M. Abrams and S. H. Strogatz, "Chimera states for coupled oscillators," Phys. Rev. Lett. **93**, 174102 (2004).
[6] S. Majhi, B. K. Bera, D. Ghosh, and M. Perc, "Chimera states in neuronal networks: A review," Phys. Life Rev. **28**, 100–121 (2019).
[7] F. Parastesh, S. Jafari, H. Azarnoush, Z. Shahriari, Z. Wang, S. Boccaletti, and M. Perc, "Chimeras," Phys. Rep. **898**, 1–114 (2021).
[8] A. Calim, J. J. Torres, M. Ozer, and M. Uzuntarla, "Chimera states in hybrid coupled neuron populations," Neural Netw. **126**, 108–117 (2020).
[9] A. Calim, P. Hövel, M. Ozer, and M. Uzuntarla, "Chimera states in networks of type-I Morris-Lecar neurons," Phys. Rev. E **98**, 062217 (2018).
[10] S. H. Strogatz, "From Kuramoto to Crawford: Exploring the onset of synchronization in populations of coupled oscillators," Phys. D: Nonlinear Phenom. **143**, 1–20 (2000).
[11] S. Boccaletti, "The synchronized dynamics of complex systems," Monogr. Ser. Nonlinear Sci. Complex. **6**, 1–239 (2008).
[12] P. Holme and J. Saramäki, "Temporal networks," Phys. Rep. **519**, 97–125 (2012).
[13] A. Buscarino, M. Frasca, L. V. Gambuzza, and P. Hövel, "Chimera states in time-varying complex networks," Phys. Rev. E **91**, 022817 (2015).
[14] D. Ghosh, M. Frasca, A. Rizzo, S. Majhi, S. Rakshit, K. Alfaro-Bittner, and S. Boccaletti, "The synchronized dynamics of time-varying networks," Phys. Rep. **949**, 1–63 (2022).
[15] B. Kerr, M. A. Riley, M. W. Feldman, and B. J. Bohannan, "Local dispersal promotes biodiversity in a real-life game of rock–paper–scissors," Nature **418**, 171–174 (2002).
[16] C. Song, Z. Qu, N. Blumm, and A.-L. Barabási, "Limits of predictability in human mobility," Science **327**, 1018–1021 (2010).
[17] T. Gross, C. J. D. D'Lima, and B. Blasius, "Epidemic dynamics on an adaptive network," Phys. Rev. Lett. **96**, 208701 (2006).
[18] D. O'Brien, "Analysis of the internal arrangement of individuals within crustacean aggregations (Euphausiacea, Mysidacea)," J. Exp. Mar. Biol. Ecol. **128**, 1–30 (1989).
[19] M. Porfiri, D. J. Stilwell, E. M. Bollt, and J. D. Skufca, "Random talk: Random walk and synchronizability in a moving neighborhood network," Phys. D: Nonlinear Phenom. **224**, 102–113 (2006).
[20] M. Frasca, A. Buscarino, A. Rizzo, L. Fortuna, and S. Boccaletti, "Synchronization of moving chaotic agents," Phys. Rev. Lett. **100**, 044102 (2008).
[21] N. Fujiwara, J. Kurths, and A. Díaz-Guilera, "Synchronization in networks of mobile oscillators," Phys. Rev. E **83**, 025101 (2011).
[22] S. Majhi and D. Ghosh, "Amplitude death and resurgence of oscillation in networks of mobile oscillators," Europhys. Lett. **118**, 40002 (2017).
[23] D. J. Stilwell, E. M. Bollt, and D. G. Roberson, "Sufficient conditions for fast switching synchronization in time-varying network topologies," SIAM J. Appl. Dyn. Syst. **5**, 140–156 (2006).
[24] S. Rakshit, B. K. Bera, E. M. Bollt, and D. Ghosh, "Intralayer synchronization in evolving multiplex hypernetworks: Analytical approach," SIAM J. Appl. Dyn. Syst. **19**, 918–963 (2020).
[25] X. Ling, W.-B. Ju, N. Guo, C.-Y. Wu, and X.-M. Xu, "Explosive synchronization in network of mobile oscillators," Phys. Lett. A **384**, 126881 (2020).
[26] F. Xiao, L. Xie, and B. Wei, "Explosive synchronization of weighted mobile oscillators," Phys. A **596**, 127099 (2022).
[27] S. Majhi, D. Ghosh, and J. Kurths, "Emergence of synchronization in multiplex networks of mobile Rössler oscillators," Phys. Rev. E **99**, 012308 (2019).
[28] S. N. Chowdhury, S. Majhi, and D. Ghosh, "Distance dependent competitive interactions in a frustrated network of mobile agents," IEEE Trans. Netw. Sci. Eng. **7**, 3159–3170 (2020).
[29] V. Nguefoue, T. Njougouo, P. Louodop, H. Fotsin, and H. A. Cerdeira, "Network of mobile systems: Mutual influence of oscillators and agents," Eur. Phys. J. Spec. Top. **231**, 237–245 (2022).
[30] T. Vicsek, A. Czirók, E. Ben-Jacob, I. Cohen, and O. Shochet, "Novel type of phase transition in a system of self-driven particles," Phys. Rev. Lett. **75**, 1226 (1995).
[31] A. Buscarino, L. Fortuna, M. Frasca, and S. Frisenna, "Interaction between synchronization and motion in a system of mobile agents," Chaos **26**, 116302 (2016).
[32] D. Levis, I. Pagonabarraga, and B. Liebchen, "Activity induced synchronization: Mutual flocking and chiral self-sorting," Phys. Rev. Res. **1**, 023026 (2019).
[33] K. P. O'Keeffe, H. Hong, and S. H. Strogatz, "Oscillators that sync and swarm," Nat. Commun. **8**, 1504 (2017).
[34] G. K. Sar, S. N. Chowdhury, M. Perc, and D. Ghosh, "Swarmalators under competitive time-varying phase interactions," New J. Phys. **24**, 043004 (2022).
[35] G. K. Sar and D. Ghosh, "Dynamics of swarmalators: A pedagogical review," Europhys. Lett. **139**, 53001 (2022).
[36] G. K. Sar, D. Ghosh, and K. O'Keeffe, "Pinning in a system of swarmalators," Phys. Rev. E **107**, 024215 (2023).
[37] C. Zhou and J. Kurths, "Noise-induced phase synchronization and synchronization transitions in chaotic oscillators," Phys. Rev. Lett. **88**, 230602 (2002).
[38] R. Toral, C. R. Mirasso, E. Hernández-Garcıa, and O. Piro, "Analytical and numerical studies of noise-induced synchronization of chaotic systems," Chaos **11**, 665–673 (2001).
[39] E. Shajan, M. P. Asir, S. Dixit, J. Kurths, and M. D. Shrimali, "Enhanced synchronization due to intermittent noise," New J. Phys. **23**, 112001 (2021).
[40] D. He, P. Shi, and L. Stone, "Noise-induced synchronization in realistic models," Phys. Rev. E **67**, 027201 (2003).
[41] M. Uzuntarla, J. J. Torres, A. Calim, and E. Barreto, "Synchronization-induced spike termination in networks of bistable neurons," Neural Netw. **110**, 131–140 (2019).
[42] S. Guan, Y.-C. Lai, C.-H. Lai, and X. Gong, "Understanding synchronization induced by "common noise"," Phys. Lett. A **353**, 30–33 (2006).
[43] F. Sivrikaya and B. Yener, "Time synchronization in sensor networks: A survey," IEEE Netw. **18**, 45–50 (2004).
[44] M. L. Sichitiu and C. Veerarittiphan, "Simple, accurate time synchronization for wireless sensor networks," in *2003 IEEE Wireless Communications and Networking, 2003 (WCNC 2003)* (IEEE, 2003), Vol. 2, pp. 1266–1273.
[45] A. Pikovskii and M. Rabinovich, "A simple autogenerator with stochastic behaviour," Dokl. Akad. Nauk SSSR **239**, 301–304 (1978).
[46] P. J. Menck, J. Heitzig, N. Marwan, and J. Kurths, "How basin stability complements the linear-stability paradigm," Nat. Phys. **9**, 89–92 (2013).
[47] C. E. Shannon, "A mathematical theory of communication," Bell Syst. Tech. J. **27**, 379–423 (1948).
[48] J. L. Hindmarsh and R. M. Rose, "A model of neuronal bursting using three coupled first order differential equations," Proc. R. Soc. Lond. Ser. B. **221**, 87–102 (1984).
[49] M. D. McDonnell and L. M. Ward, "The benefits of noise in neural systems: Bridging theory and experiment," Nat. Rev. Neurosci. **12**, 415–425 (2011).
[50] A. N. Pisarchik and A. E. Hramov, "Coherence resonance in neural networks: Theory and experiments," Phys. Rep. **1000**, 1–57 (2023).
[51] C.-H. Lai and C. Zhou, "Synchronization of chaotic maps by symmetric common noise," Europhys. Lett. **43**, 376 (1998).